



Full paper/Mémoire

Tetrathiafulvalene-based lanthanide coordination complexes: Synthesis, crystal structure, optical and electrochemical characterization

Ying-Fen Ran^a, Martin Steinmann^a, Marc Sigrist^{b,c}, Shi-Xia Liu^{a,*}, Jürg Hauser^a, Silvio Decurtins^a

^a *Departement für Chemie und Biochemie, Universität Bern, Freiestrasse 3, CH-3012 Bern, Switzerland*

^b *Institute Laue Langevin, avenue des Martyrs, BP 156, 38042 Grenoble cedex 9, France*

^c *Institute of Chemistry, Universitetsparken 5, DK-2100 Copenhagen, Denmark*

ARTICLE INFO

Article history:

Received 15 December 2011

Accepted after revision 20 March 2012

Available online 7 May 2012

Keywords:

Lanthanide complexes

Tetrathiafulvalene

X-ray crystal structure

Electrochemistry

Magnetic susceptibility

Charge transfer

ABSTRACT

The explorative lanthanide coordination chemistry of 4',5'-bis-(propylthio)tetrathiafulvenyl[i]dipyrido[3,2-*a*:2',3'-*c*]phenazine (TTF-dppz) is described. Thereby, four new Ln(III) complexes, [Ln(NO₃)₃(TTF-dppz)₂] with Ln(III) = Nd (**1**), Eu (**2**), Gd (**3**), Tb (**4**), have been prepared and characterized. An X-ray crystallographic study of [Gd(NO₃)₃(TTF-dppz)₂] (**3**) shows that the Gd(III) ion is coordinated to six oxygen atoms from three bidentate nitrate ligands and four nitrogen atoms from two bidentate TTF-dppz molecules forming a distorted bicapped square antiprism coordination geometry. The UV-vis spectra of the four Ln(III) complexes show very strong absorption bands in the UV region consistent with ligand centred electronic π - π^* transitions and an intense broad absorption band in the visible region corresponding to a spin-allowed electronic π - π^* ¹ILCT transition from the TTF-dppz ligand. Upon coordination, the ¹ILCT band of the free TTF-dppz ligand is bathochromically shifted. The electrochemical studies reveal that all complexes undergo two reversible oxidation and one (quasi)reversible reduction processes, ascribed to the successive oxidations of the TTF moiety and the reduction of the dppz unit, respectively. Moreover, the magnetic properties of complexes **3** and **4** are discussed.

© 2012 Académie des sciences. Published by Elsevier Masson SAS. All rights reserved.

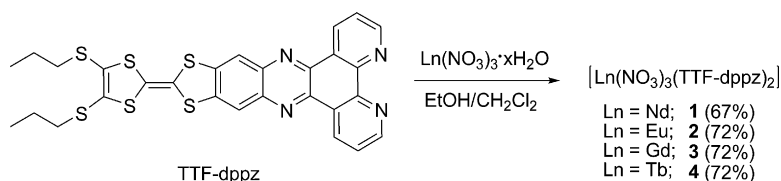
1. Introduction

The search for molecule-based materials exhibiting multiphysical properties is one of the current challenges in molecular materials science [1,2]. Great interest is currently devoted to obtain organic/inorganic hybrid materials in which it is expected that there is long-range magnetic coupling between the localised spins on *d*-orbitals of the paramagnetic transition metal ions of the inorganic part through the mobile electrons of the conducting networks (π -electrons) formed by the organic ligands [1,3,4]. To achieve strong interactions between the paramagnetic metal ions and, for example, the

redox-active tetrathiafulvalene (TTF) ligands, the strategy which involves the covalent attachment of metal ion binding groups to π -conjugated TTF derivatives and their linkage into supramolecular systems, has been investigated. With the appropriate choice of metal ions, the resulting systems would be expected to show multiple physical properties, such as electrical conductivity or superconductivity and magnetic effects, optical and magnetic properties or spin-crossover, in a synergistic way. Within this context, the binding of 4',5'-bis-(propylthio)tetrathiafulvenyl[i]dipyrido[3,2-*a*:2',3'-*c*]phenazine (TTF-dppz) and its analogue 4',5'-bis(propylthio)tetrathiafulvenyl[i]dipyrido[2,3-*a*:3',2'-*c*]phenazine (TTF-ppb) to a variety of transition metal ions and their excited-state charge separation characteristics have been investigated in our laboratory [5]. Herein, we now describe the synthesis of four new lanthanide complexes (**1-4**) with the TTF-dppz

* Corresponding author.

E-mail address: liu@iac.unibe.ch (S.-X. Liu).



Scheme 1. A synthetic route for the preparation of complexes **1–4**.

ligand (**Scheme 1**), together with their electrochemical, optical and magnetic properties as well as the crystal structure of the corresponding Gd(III) complex, namely $[\text{Gd}(\text{NO}_3)_3(\text{TTF-dppz})_2]$ (**3**).

Compared to the numerous studies on coordination compounds composed of *d*-metal ions and TTF-type ligands, the investigations on corresponding lanthanide complexes are quite rare [6]. In fact, lanthanide compounds are appealing, e.g. by virtue of their specific luminescence, *f*-electron configurations, nonlinear optics and magnetic characteristics [7,8]. On the one hand, it has been demonstrated that TTF-based ligands act as efficient charge transfer antennae for the sensitization of Yb(III) NIR luminescence [6a,b]. On the other hand, Ouahab et al. reported that a dinuclear Dy(III) complex bearing two electroactive functionalized TTFs behaves as a single-molecule magnet with an energy barrier, in zero magnetic field, as high as 87 K [6f]. During this work, we have explored the coordination ability of TTF-dppz to some lanthanide(III) ions in order to establish a new combination of Ln(III) ions with π -extended redox-active chromophoric ligands.

2. Results and discussion

2.1. Syntheses

The molecule TTF-dppz was synthesized according to the literature procedure [5a] and $[\text{Gd}(\text{III})(\text{NO}_3)_3] \cdot 6\text{H}_2\text{O}$ was prepared by evaporation of an aqueous solution of

gadolinium oxide in the presence of nitric acid. $[\text{Nd}(\text{III})(\text{NO}_3)_3] \cdot 6\text{H}_2\text{O}$, $[\text{Eu}(\text{III})(\text{NO}_3)_3] \cdot 6\text{H}_2\text{O}$ and $[\text{Tb}(\text{III})(\text{NO}_3)_3] \cdot 5\text{H}_2\text{O}$ are commercial products. The lanthanide(III) complexes $[\text{Ln}(\text{NO}_3)_3(\text{TTF-dppz})_2]$ with Ln(III) = Nd (**1**), Eu (**2**), Gd (**3**), Tb (**4**) were obtained following a general synthetic procedure as shown in **Scheme 1**. To a solution of TTF-dppz ligand (2 equiv.) in CH_2Cl_2 was added a solution of $[\text{Ln}(\text{III})(\text{NO}_3)_3] \cdot x\text{H}_2\text{O}$ (1 equiv.) in ethanol. The color of the solution changed from red purple to blue, immediately followed by the precipitation of the heteroleptic Ln(III) complexes. All complexes are stable in the solid state and can be isolated as deep-blue powders in good yields after washing with a large amount of ethanol and drying in vacuum. Single crystals of **3** were grown by slow diffusion of hexane to its CH_2Cl_2 solution in the dark.

2.2. Crystal structure of complex **3**

Complex **3** crystallizes in the orthorhombic polar space group *Fdd2* as an inversion twin with a component ratio of 0.625(10)/0.375(10). It is composed of a Gd(III) ion coordinated with three nitrate ligands and two TTF-dppz molecules. There are four complexes per asymmetric unit and thus 64 complexes in the huge unit cell. One bis-propylthio-TTF fragment is disordered over two conformations with a site population ratio of 0.436/0.564. One propylthio group has 0.5/0.5 disorder over two sites. **Fig. 1** shows one of the four crystallographically independent complexes. The Gd atom is coordinated by four N atoms of two TTF-dppz ligands and six O atoms of three nitrate

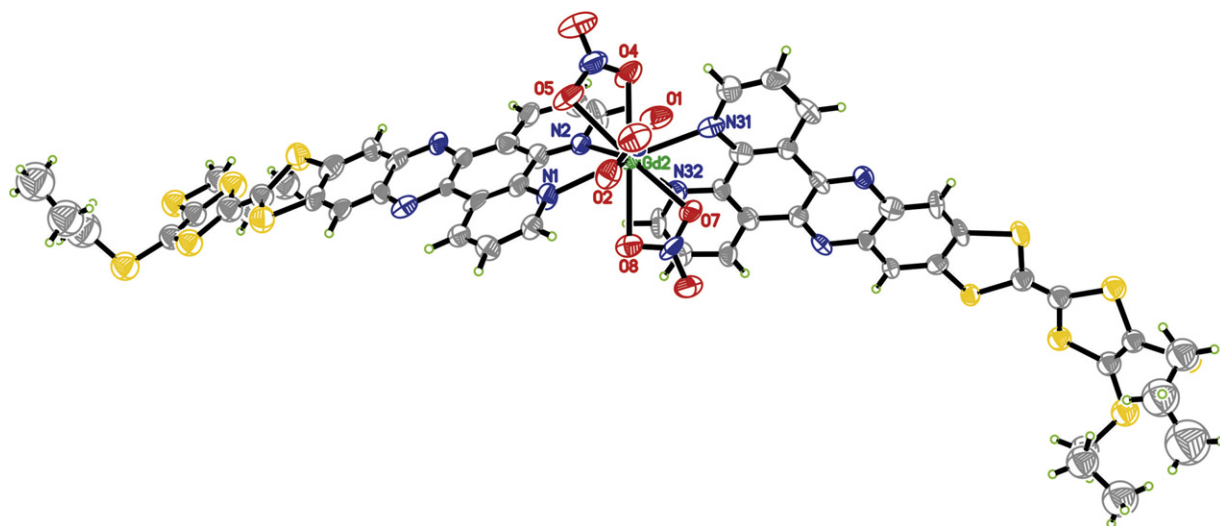


Fig. 1. ORTEP representation [12] of the molecular structure of complex **3**; view of one of the four independent complexes (30% probability ellipsoids; H-atoms given arbitrary displacement parameters for clarity). The atoms at the vertices of the bicapped square antiprism are labeled.

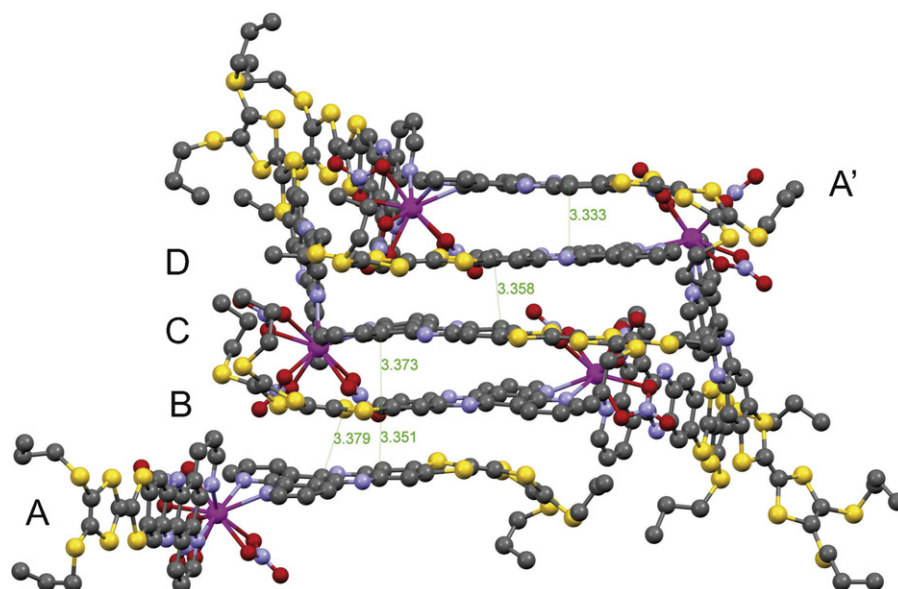


Fig. 2. Crystal packing pattern of **3**; stacking of the TTF-dppz ligands along [01–1] (interatomic distances given in Å, H-atoms are omitted for clarity).

ligands to form a 10-fold coordination which may be seen as a distorted bicapped square antiprism (top square: O1/O5/N2/N31; bottom square: O2/O7/N32/N1; capped by O4 and O8). One nitrate ligand bridges from the top cap to the upper square (O4/O5), and a second one bridges from the lower cap to the lower square (O8/O7); the third nitrate ligand as well as the two TTF-dppz molecules connect the upper with the lower square (O1/O2, N2/N1 and N31/N32). The ranges of bond distances for the four complexes are 2.488(14)–2.628(12) Å, 2.562(14)–2.614(13) Å, 2.537(13)–2.598(14) Å, 2.571(14)–2.617(14) Å for Gd–N and 2.418(11)–2.583(10) Å, 2.476(11)–2.526(11) Å, 2.459(12)–2.504(13) Å, 2.428(12)–2.575(15) Å for Gd–O, respectively, indicating that their coordination geometries are similar but have slightly different distortions. The mean Gd–N bond distances of the four complexes of 2.54(6) Å, 2.58(3) Å, 2.57(2) Å and 2.59(6) Å are slightly longer than the mean Gd–O bond distances of 2.50(7) Å, 2.499(19) Å, 2.473(13) Å and 2.48(5) Å. They match the corresponding mean distances of the closely related $[\text{Gd}(\text{NO}_3)_3(\text{phen})_2]$ [9] of 2.54(3) Å and

2.51(3) Å. The TTF-dppz ligands are stacked head-to-tail along the [01–1] and $[0\bar{1}\bar{1}]$ directions with their molecular planes almost parallelly aligned (Fig. 2). Ligands A and B have nearly perfect antiparallel orientations. The other ligand pairs, C and D, are aligned in a crossed orientation. The shortest contacts between atoms in neighbouring ligand planes are S61–C131 3.379 Å, C76–C138 3.351 Å, C4–C76 3.373 Å, C227–C17 3.358 Å and C138–C222 3.333 Å and thus indicate a pronounced π – π stacking effect. The only S–S contact which is shorter than the sum of the v.d.W. radii is S32–S186 with 3.563 Å.

2.3. Electrochemical studies

The electrochemical properties of the lanthanide(III) complexes **1–4** in CH_2Cl_2 were investigated by cyclic voltammetry as illustrated in Fig. 3. Their cyclic voltammetric data are collected in Table 1 together with those of the TTF-dppz ligand for comparison. In each case, two reversible single-electron oxidation waves around 0.83

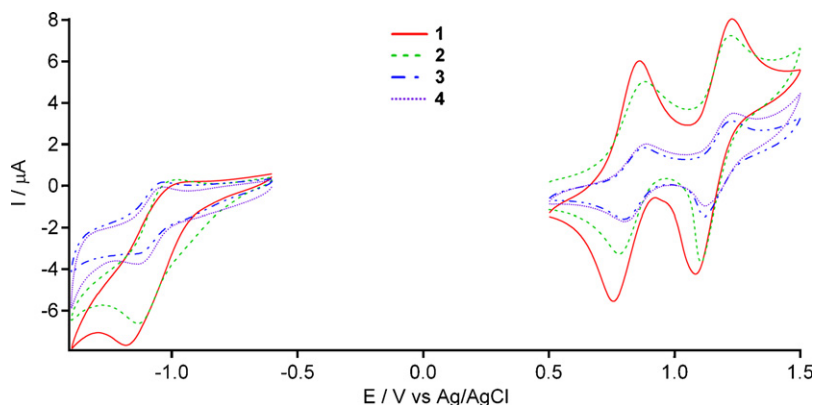


Fig. 3. Cyclic voltammograms of **1–4** in CH_2Cl_2 .

Table 1
Cyclic voltammetric data.^a

<i>E</i> /V	<i>E</i> _{1/2} ^{red1}	<i>E</i> _{1/2} ^{ox1}	<i>E</i> _{1/2} ^{ox2}
TTF-dppz	−1.17	0.73	1.08
1	−1.08 ^a	0.81	1.16
2	−1.06	0.83	1.16
3	−1.08	0.84	1.17
4	−1.08	0.84	1.17

^a Conditions: all oxidation potentials were determined in CH₂Cl₂ under Ar at r.t. containing 0.1 M Bu₄N(PF₆), with Ag/AgCl as reference electrode, Pt disk as working electrode and glassy carbon as counter electrode, scan rate 100 mV s^{−1}.

and 1.17 V are observed, both typical of the TTF unit (see: *E*_{1/2}^{ox1} and *E*_{1/2}^{ox2} in Table 1). In the negative potential direction, one (quasi)-reversible reduction is observed corresponding to the reduction of the dppz moiety of the ligand. Upon coordination, both oxidation and reduction potentials are positively shifted by 100 mV due to the electron-withdrawing effect of the lanthanide(III) ions.

2.4. Optical properties

The electronic absorption spectra of the lanthanide(III) complexes **1–4** were determined in CH₂Cl₂ solution, as shown in Fig. 4. The key feature of the absorption spectra is

the intense broad absorption band which appears for all four compounds around 18,000 cm^{−1} (555 nm). This optical absorption band can be readily attributed to a spin-allowed electronic π–π* intraligand charge-transfer transition (¹ILCT) which is based on the TTF subunit as an electron donor and the dppz subunit as an electron acceptor; this electronic transition is well documented in case of the optical absorption spectrum of the free TTF-dppz ligand [5a]. Compared to the free ligand, the ¹ILCT bands for the complexes **1–4** are red-shifted by about 700 cm^{−1}, a fact which is also well documented for other metal complexes with the TTF-dppz ligand [5b]. At energies higher than 25,000 cm^{−1} (400 nm), the optical absorptions correspond mainly to electronic π–π* transitions of the dppz units.

2.5. Magnetic properties of complexes 3 and 4

Among the four mononuclear paramagnetic lanthanide(III) compounds presented herein, the complexes **3** and **4** have been selected for an investigation by magnetic SQUID measurements. These two representative examples will demonstrate that this type of mononuclear complexes exhibit predictable magnetic signatures. In the case of **3**, the thermal variation of χ_MT together with the inverse susceptibility vs temperature curve and the magnetization data are presented in Fig. 5. The χ_MT product exhibits a

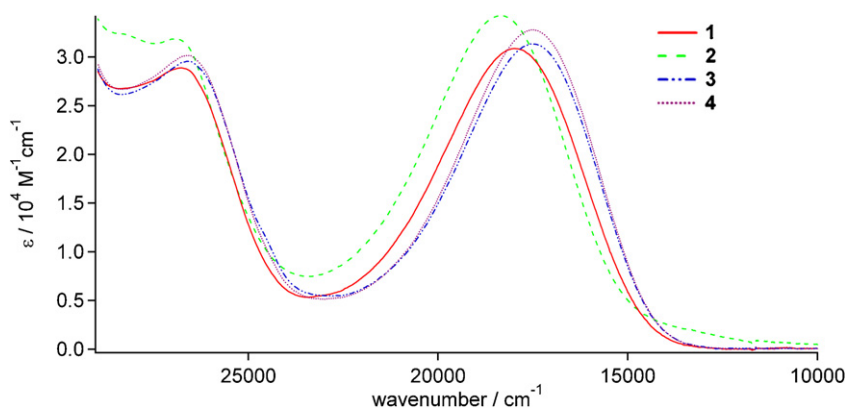


Fig. 4. Electronic absorption spectra of **1–4** in CH₂Cl₂.

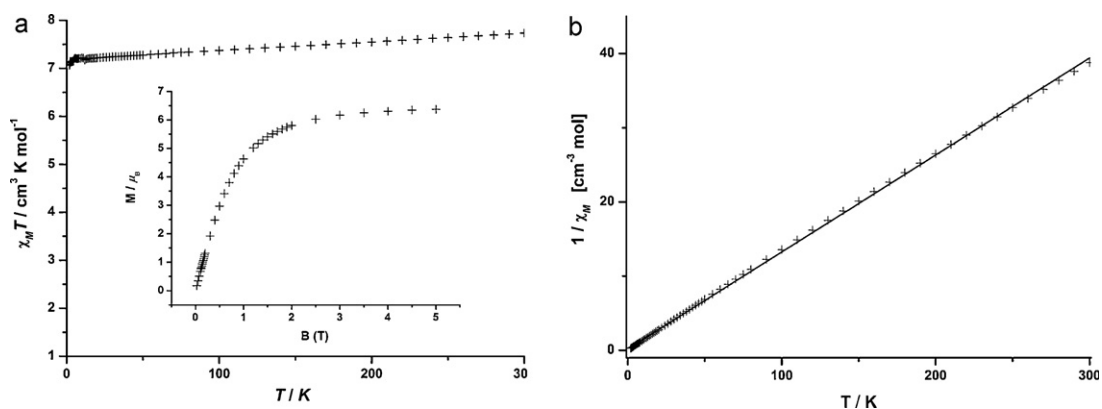


Fig. 5. a: thermal variation of χ_MT and magnetization versus field at 1.9 K (inset) for **3**; b: inverse magnetic susceptibility versus temperature (solid line is a fit from 50 to 290 K) for **3**.

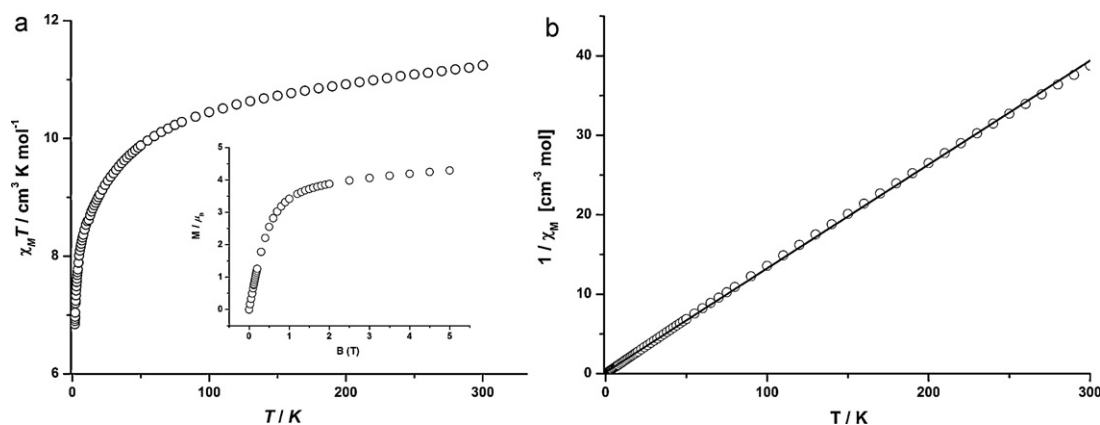


Fig. 6. a: thermal variation of $\chi_M T$ and magnetization versus field at 1.9 K (inset) for **4**; b: inverse magnetic susceptibility versus temperature (solid line is a fit from 50 to 290 K) for **4**.

value of $7.74 \text{ cm}^3 \text{ K mol}^{-1}$ at room temperature which is very close to the expected value of $7.88 \text{ cm}^3 \text{ K mol}^{-1}$ for the spin-only center of a Gd(III) ion with an $^8S_{7/2}$ ground state ($S = 7/2, g = 2$) [8]. Since there is no spin-orbit coupling and the first electronic excited state is about $30,000 \text{ cm}^{-1}$ above the ground state, no deviation from the Curie law is expected and accordingly, the experimental $\chi_M T$ values stay practically constant over the whole temperature range. Similarly, the inverse susceptibility curve shows a linear behaviour in the temperature range from 50 to 290 K and the Curie constant C gives a value of $61.5 N\beta^2/3k$, what compares well with the theoretical value $63.0 N\beta^2/3k$. The magnetization data which are taken at 1.9 K reach a magnetic moment value of $6.37 \mu_B$ with a magnetic field of 5 T; this value is already quite close to the theoretical saturation value of $7 \mu_B$.

Fig. 6 illustrates the magnetic behaviour of complex **4** including the $\chi_M T(T)$ curve, the inverse susceptibility vs temperature curve and the magnetization data. The Tb(III) ion is described with a 7F_6 ground state ($S = 3, L = 3, J = 6, g_J = 3/2$), thus the theoretical $\chi_M T$ value is $11.82 \text{ cm}^3 \text{ K mol}^{-1}$. At room temperature, the experimental $\chi_M T$ value is $11.25 \text{ cm}^3 \text{ K mol}^{-1}$, which is close to the theoretical one. For Tb(III), the first electronic excited multiplet is separated by more than 1000 cm^{-1} from the ground state and importantly, the latter is split in Stark sub-levels; the relevant crystal field effects are of the order of 100 cm^{-1} . Consequently, a deviation from the Curie law is expected through a depopulation of these sub-levels when the temperature is decreased. Accordingly, the experimental $\chi_M T$ values decrease continually while lowering the temperature. A fit over the 50 to 290 K temperature range of the inverse susceptibility data revealed a C value of $88.9 N\beta^2/3k$ ($94.5 N\beta^2/3k$ in theory). The magnetization data which are taken at 1.9 K show a magnetic moment value of $4.33 \mu_B$ with a magnetic field of 5 T, close to a saturation value.

3. Conclusion

In conclusion, four new lanthanide complexes with the π -conjugated redox-active chromophoric TTF-dppz ligand

were synthesized and characterized. They form stable and well defined complexes exhibiting an intense colour. Further studies to probe the TTF-dppz ligand as an antenna for the sensitization of NIR emitters also in function of the redox states of the ligand is in progress in our laboratory.

4. Experimental

4.1. Synthesis

4.1.1. General methods and instrumentation

Unless stated otherwise, all reagents were purchased from commercial sources and used without additional purification. The compound 4',5'-bis-(propylthio)tetrathiafulvenyl[*i*]dipyrido[3,2-*a*:2',3'-*c*]phenazine (TTF-dppz) was prepared according to literature procedure [5a]. Elemental analyses were performed on an EA 1110 Elemental Analyzer CHN Carlo Erba Instruments. FTIR data was collected on a Perkin-Elmer Spectrum One spectrometer at a resolution of 4 cm^{-1} . Cyclic voltammetric measurements were conducted on a VA-Stand 663 electrochemical analyzer.

4.1.2. Lanthanide complexation procedure

To a solution of $[\text{Ln}(\text{NO}_3)_3] \cdot x\text{H}_2\text{O}$ ($\text{Ln}(\text{III}) = \text{Nd, Eu, Gd, Tb}$) (1 equiv.) in ethanol (10 mL) in a 50 mL beaker was added a solution of 4',5'-bis-(propylthio)tetrathiafulvenyl[*i*]dipyrido[3,2-*a*:2',3'-*c*]phenazine (TTF-dppz) ligand (2 equiv.) in CH_2Cl_2 (5 mL). The resulting deep blue mixture was stirred for 3 h at r.t. A deep blue precipitate was immediately formed, filtered off and washed with ethanol ($3 \times 20 \text{ mL}$). The collected solid was dried under vacuum to afford the corresponding target complex as a deep blue powder.

$[\text{Nd}(\text{NO}_3)_3(\text{TTF-dppz})_2]$ (**1**). Yield: 52.7 mg (66.9%); IR (KBr, cm^{-1}): 2958, 2926, 1638, 1486, 1400, 1384, 1287, 1088, 737; Anal. calcd for $\text{C}_{56}\text{H}_{44}\text{N}_{11}\text{NdO}_9\text{S}_{12}$: C, 43.56; H, 2.87; N, 9.98. Found: C, 43.29; H, 2.93; N, 9.62.

$[\text{Eu}(\text{NO}_3)_3(\text{TTF-dppz})_2]$ (**2**). Yield: 53.6 mg (72.1%); IR (KBr, cm^{-1}): 2962, 2926, 1631, 1486, 1400, 1384, 1291, 1089, 737; Anal. calcd for $\text{C}_{56}\text{H}_{44}\text{EuN}_{11}\text{O}_9\text{S}_{12} \cdot \text{H}_2\text{O}$: C, 42.85; H, 2.95; N, 9.68. Found: C, 42.79; H, 2.87; N, 9.43.

[Gd(NO₃)₃(TTF-dppz)₂] (**3**). Yield: 66.8 mg (72.0%); IR (KBr, cm⁻¹): 2959, 2922, 1656, 1486, 1401, 1384, 1290, 1088, 737; Anal. calcd for C₅₆H₄₄GdN₁₁O₉S₁₂: C, 43.20; H, 2.85; N, 9.90. Found: C, 42.88; H, 2.87; N, 9.72.

[Tb(NO₃)₃(TTF-dppz)₂] (**4**). Yield: 61.3 mg (65.3%); IR (KBr, cm⁻¹): 2958, 2929, 1631, 1487, 1400, 1384, 1291, 1089, 737; Anal. Calcd (%) for C₅₆H₄₄N₁₁O₉S₁₂Tb: C, 43.15; H, 2.85; N, 9.24. Found: C, 43.14; H, 2.91; N, 9.47.

4.2. X-ray crystallography

X-ray data were measured on an Oxford Diffraction SuperNova area-detector diffractometer using mirror optics monochromated Mo K α radiation ($\lambda = 0.71073 \text{ \AA}$). The crystal was non-merohedrally twinned with a minor twin component of 10%. Data reduction was performed only on the reflections of the major twin component using the CrysAlisPro program [10]. The intensities were corrected for Lorentz and polarization effects, and an absorption correction based on the multi-scan method using SCALE3 ABSPACK routine in CrysAlisPro [10] was applied. The crystal did not scatter to higher resolution ranges, i.e. the mean $1/\sigma(I)$ drops to 2.16 in the resolution range 0.98–0.93 \AA . The structure was solved by direct methods using SIR92 [11], which revealed the positions of only a part of the non-hydrogen atoms. One bis-propylthio-TTF fragment is disordered over two conformations with a population ratio of 0.436/0.564. One propylthio group is 0.5/0.5 disordered over two sites. All other propylthio groups have large adp's but no disorder model could be derived. The 1,2 and 1,3 distances of all disordered fragments and of all propylthio groups were restrained to the distances of the free ligand [5a]. The

adp's of all disordered atoms and the ones of the propylthio groups were kept isotropic and were restrained to be similar (SHELX SIMU instruction). The non-hydrogen and not disordered atoms were refined anisotropically, but their adp's had to be restrained by the SHELX ISOR instruction. The H-atoms were placed in geometrically calculated positions and refined using a riding model where each H-atom was assigned a fixed isotropic displacement parameter with a value equal to 1.2 Ueq of its parent atom (1.5 Ueq for the methyl groups). Refinement of the structure was carried out on F^2 using full-matrix least-squares procedures, which minimized the function $\sum w(F_o^2 - F_c^2)^2$. The weighting scheme was based on counting statistics and included a factor to down-weight the intense reflections. All calculations were performed using the SHELXL-97 program [12]. Data collection and refinement parameters are listed in Table 2.

Acknowledgment

Support for this research by the Swiss National Science Foundation (grant No. 200020-130266/1) is gratefully acknowledged. The X-ray diffraction analysis was possible thanks to the Swiss National Science Foundation (R'Equip project 206021_128724).

Supplementary material

Crystallographic data have been deposited with the Cambridge Crystallographic Data Centre, 12 Union Road, Cambridge CB2 1EZ, UK, as supplementary material No. SUP 857998 and can be obtained by contacting the CCDC (fax: +44 1223 336 033; deposit@ccdc.cam.ac.uk).

Table 2
Crystal data and structure refinement for **3**.

Empirical formula	C ₅₆ H ₄₄ GdN ₁₁ O ₉ S ₁₂
Formula weight	1556.99
Temperature	173(2) K
Wavelength	0.71073 \AA
Crystal system	Orthorhombic
Space group	F d d 2
Unit cell dimensions	$a = 56.3714(8) \text{ \AA}$ $b = 47.6098(6) \text{ \AA}$ $c = 43.4418(6) \text{ \AA}$
Volume	116590(3) \AA^3
Z, Z'	64, 4
Density (calculated)	1.419 Mg/m ³
Absorption coefficient	1.31 mm ⁻¹
F(000)	50240
Crystal size	0.292 \times 0.103 \times 0.073 mm ³
Theta range for data collection	1.46 to 26.04 $^\circ$
Index ranges	$-69 \leq h \leq 68$, $-58 \leq k \leq 58$, $-52 \leq l \leq 53$
Reflections collected	259053
Independent reflections	53903 [R(int) = 0.0692]
Completeness to theta = 25 $^\circ$	99.8%
Max. and min. transmission	1 and 0.93075
Refinement method	Full-matrix least-squares on F^2
Data/restraints/parameters	53903/1881/2680
Goodness-of-fit on F^2	1.667
Final R indices [$I > 2\sigma(I)$]	$R_1 = 0.1062$, $wR_2 = 0.249$
R indices (all data)	$R_1 = 0.1672$, $wR_2 = 0.2665$
Largest diff. peak and hole	1.195 and $-0.969 \text{ e-\AA}^{-3}$

References

- [1] (a) J.L. Segura, N. Martín, *Angew. Chem. Int. Ed.* 40 (2001) 1372; (b) D. Lorcý, N. Bellec, M. Fourmigué, N. Avarvari, *Coord. Chem. Rev.* 253 (2009) 1398; (d) S. Rabaça, M. Almeida, *Chem. Rev.* 254 (2010) 1493; (e) L. Ouahab, T. Enoki, *Eur. J. Inorg. Chem.* (2004) 933; (f) M. Fourmigué, L. Ouahab (Eds.), *Conducting and Magnetic Organometallic Molecular Materials*, Springer, Heidelberg, 2009; (g) F. Pointillart, T. Cauchy, Y. Le Gal, S. Golhen, O. Cador, L. Ouahab, *Inorg. Chem.* 49 (2010) 1947; (h) D. Canevet, M. Sallé, G. Zhang, D. Zhang, D. Zhu, *Chem. Commun.* (2009) 2245; (i) J.I. Yamada, T. Sugimoto (Eds.), *TTF Chemistry: Fundamentals and Applications of Tetrathiafulvalene*, Springer, Berlin, 2004.
- [2] (a) H. Shinagawa, T. Terashima, C. Terakura, T. Yakabe, Y. Terai, M. Tokumoto, A. Kobayashi, H. Tanaka, H. Kobayashi, *Nature* 410 (2001) 908; (b) V. Khodorkovsky, J.Y. Becker, in: J.P. Farges (Ed.), *Organic Conductors: Fundamentals and Applications*, Marcel Dekker, New York, 1994, Chapter 3, p. 75; (c) For reviews on this topic, see special issue on molecular conductors: P. Batail, Guest Editor. *Chem. Rev.* 104 (2004) 4887.
- [3] (a) T. Devic, N. Avarvari, P. Batail, *Chem. Eur. J.* 10 (2004) 3697; (b) S. Golhen, O. Cador, L. Ouahab, *Dalton Trans.* (2009) 3495; (c) K. Hervé, S.X. Liu, O. Cador, S. Golhen, Y. Le Gal, A. Bousseksou, H. Stoeckli-Evans, S. Decurtins, L. Ouahab, *Eur. J. Inorg. Chem.* (2006) 3498; (d) J. Massue, N. Bellec, S. Chopin, E. Levillain, T. Roisnel, R. Clérac, D. Lorcý, *Inorg. Chem.* 44 (2005) 8740; (e) P. Pellon, G. Gachot, J. Le Bris, S. Marchin, R. Carlier, D. Lorcý, *Inorg. Chem.* 42 (2003) 2056; (f) T. Devic, P. Batail, M. Fourmigué, N. Avarvari, *Inorg. Chem.* 43 (2004) 3136; (g) N. Avarvari, M. Fourmigué, *Chem. Commun.* (2004) 1300;

- (h) F. Iwahori, S. Golhen, L. Ouahab, R. Carlier, J.P. Sutter, *Inorg. Chem.* 40 (2001) 6541;
- (i) S. Ichikawa, S. Kimura, H. Mori, G. Yoshida, H. Tajima, *Inorg. Chem.* 45 (2006) 7575;
- (j) L. Wang, B. Zhang, J. Zhang, *Inorg. Chem.* 45 (2006) 6860;
- (k) K.S. Gavrilenko, Y. Le Gal, O. Cador, S. Golhen, L. Ouahab, *Chem. Commun.* (2007) 280;
- (l) F. Pointillart, Y. Le Gal, S. Golhen, O. Cador, L. Ouahab, *Inorg. Chem.* 47 (2008) 9730;
- (m) Y. Umezono, W. Fujita, K. Awaga, *J. Am. Chem. Soc.* 128 (2006) 1084;
- (n) Z.J. Lu, J.P. Wang, Q.Y. Zhu, L.B. Huo, Y.R. Qin, J. Dai, *Dalton Trans.* 39 (2010) 2798;
- (o) M. Nihei, N. Takahashi, H. Nishikawa, H. Oshio, *Dalton Trans.* 40 (2011) 2154.
- [4] (a) S.X. Liu, S. Dolder, E.B. Rusanov, H. Stoeckli-Evans, S. Decurtins, *Chimie C. R.* 6 (2003) 657;
- (b) S.X. Liu, S. Dolder, M. Pilkington, S. Decurtins, *J. Org. Chem.* 67 (2002) 3160;
- (c) S.X. Liu, S. Dolder, P. Franz, A. Neels, H. Stoeckli-Evans, S. Decurtins, *Inorg. Chem.* 42 (2003) 4801;
- (d) C. Jia, S.X. Liu, C. Ambrus, A. Neels, G. Labat, S. Decurtins, *Inorg. Chem.* 45 (2006) 3152;
- (e) J.C. Wu, S.X. Liu, T.D. Keene, A. Neels, V. Mereacre, A.K. Powell, S. Decurtins, *Inorg. Chem.* 47 (2008) 3452;
- (f) S. Dolder, S.X. Liu, F. Le Derf, M. Sallé, A. Neels, S. Decurtins, *Org. Lett.* 9 (2007) 3753;
- (g) Y.F. Ran, C. Blum, S.X. Liu, L. Sanguinet, E. Levillain, S. Decurtins, *Tetrahedron* 67 (2011) 1623;
- (h) J. Wu, N. Dupont, S.X. Liu, A. Neels, A. Hauser, S. Decurtins, *Chem. Asian J.* 4 (2009) 392;
- (i) S.X. Liu, C. Ambrus, S. Dolder, A. Neels, S. Decurtins, *Inorg. Chem.* 45 (2006) 9622;
- (j) C.Y. Jia, S.X. Liu, C. Tanner, C. Leiggener, L. Sanguinet, E. Levillain, S. Leutwyler, A. Hauser, S. Decurtins, *Chem. Commun.* (2006) 1878.
- [5] (a) C.Y. Jia, S.X. Liu, C. Tanner, C. Leiggener, A. Neels, L. Sanguinet, E. Levillain, S. Leutwyler, A. Hauser, S. Decurtins, *Chem. Eur. J.* 13 (2007) 3804;
- (b) C. Goze, C. Leiggener, S.X. Liu, L. Sanguinet, E. Levillain, A. Hauser, S. Decurtins, *Chem. Phys. Chem.* 8 (2007) 1504;
- (c) Y.F. Ran, S.X. Liu, O. Sereda, A. Neels, S. Decurtins, *Dalton Trans.* 40 (2011) 8193;
- (d) C. Goze, N. Dupont, E. Beitler, C. Leiggener, H. Jia, P. Monbaron, S.X. Liu, A. Neels, A. Hauser, S. Decurtins, *Inorg. Chem.* 47 (2008) 11010;
- (e) N. Dupont, Y.F. Ran, H.P. Jia, J. Grilj, J. Ding, S.X. Liu, S. Decurtins, A. Hauser, *Inorg. Chem.* 50 (2011) 3295.
- [6] (a) S. Faulkner, B.P. Burton-Pye, T. Khan, L.R. Martin, S.D. Wray, P.J. Skabara, *Chem. Commun.* (2002) 1668;
- (b) F. Pointillart, T. Cauchy, O. Maury, Y. Le Gal, S. Golhen, O. Cador, L. Ouahab, *Chem. Eur. J.* 16 (2010) 11926;
- (c) F. Pointillart, Y. Le Gal, S. Golhen, O. Cador, L. Ouahab, *Chem. Commun.* (2009) 3777;
- (d) S. Golhen, O. Cador, L. Ouahab, *Inorg. Chem.* 48 (2009) 4631;
- (e) S.J.A. Pope, B.P. Burton-Pye, R. Berridge, T. Khan, P. Skabara, S. Faulkner, *Dalton Trans.* (2006) 2907;
- (f) F. Pointillart, Y. Le Gal, S. Golhen, O. Cador, L. Ouahab, *Chem. Eur. J.* 17 (2011) 10397.
- [7] (a) C. Andraud, O. Maury, *Eur. J. Inorg. Chem.* (2009) 4357;
- (b) J.C.G. Bünzli, C. Piguat, *Chem. Rev.* 102 (2002) 1897;
- (c) J. Kido, Y. Okamoto, *Chem. Rev.* 102 (2002) 2357.
- [8] C. Benelli, D. Gatteschi, *Chem. Rev.* 102 (2002) 2369.
- [9] V.B. Rybakov, V.N. Zakharov, A.L. Kamyshnyl, L.A. Aslanov, A.P. Suisalu, *Koord. Khim.* 17 (1991) 1061.
- [10] CrysAlisPro, version 1.171.35.10, Oxford Diffraction Ltd., Yarnton, Oxfordshire, UK, 2011.
- [11] A. Altomare, G. Casciarano, C. Giacovazzo, A. Guagliardi, M.C. Burla, G. Polidori, M. Camalli, *J. Appl. Crystallogr.* 27 (1994) 435.
- [12] G.M. Sheldrick, *Acta Cryst. A* 64 (2008) 112.